Ab Initio Study on the Mechanism of Tropospheric Reactions of the Nitrate Radical with Alkenes: Ethene

M. Pilar Pérez-Casany, Ignacio Nebot-Gil,* José Sánchez-Marín, and Francisco Tomás-Vert

Departament de Química Física, Facultat de Química, Universitat de València, c/Dr. Moliner, 50, 46100 Burjassot (Valencia), Spain

Ernesto Martínez-Ataz, Beatriz Cabañas-Galán, and Alfonso Aranda-Rubio

Departamento de Química Física, Facultad de Química, Universidad de Castilla-La Mancha, Campus Universitario 13071, Ciudad Real, Spain

Received April 28, 1998

A mechanism for the reaction of the NO_3 radical with the simplest alkene, ethene, is proposed. The mechanism involves three paths leading to three main different products: oxirane, ethanal, and nitric acid. The three paths start from the same initial intermediate, an NO_3−ethene adduct. The calculated energy barriers show that the oxirane is the product kinetically more favored. Initial analysis of the potential energy surface was made at AM1 level. Then, the geometries and characterization of the found stationary points on the surface were refined at ROHF level with a 6-31G* basis set. Further refinement was carried out at CASSCF level with the same basis set, and an active space was built with five active electrons in six active orbitals.

1. Introduction

Atmospheric chemistry is very important in environmental sciences because of its implications in the environment's future and economics. A lot of reactions take place in the atmosphere, and many studies are needed in order to ascertain them and establish their mechanisms. Oxidation reactions are among the most important in the lower levels of the atmosphere, due mainly to the presence in it of emissions of both organic compounds and oxidant inorganic radicals derived from human activity.

The most important oxidant agents in the troposphere are ozone and the OH and nitrate radicals.[1] The OH radical is the principal oxidant of organic compounds during daytime and the NO_3 radical during the night, because of the fast photolysis of the latter. Thus, the concentration of the NO_3 radical is maximum during the night and minimum during the daytime. The whole effect on many compounds of the NO_3 radical is greater than that of the OH radical.[1,2] Reactions of the nitrate radical with unsaturated hydrocarbons represent a significant way for the loss of these compounds in the troposphere.[1]

Kinetic and product data show that reactions of NO_3 with alkenes proceed initially via electrophilic addition of NO_3 to the carbon−carbon double bond, forming a radical adduct intermediate:

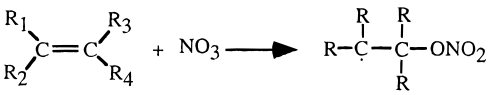

Also, it has been shown[1] that the reactions between the nitrate radical and alkenes are relatively fast, with reaction rate constants increasing with alkyl substitution.[3]

Reaction products were first analyzed by FT-IR by Morris et al.[4] and Japar et al.[5] From experiments in a smog chamber under aerobic conditions, Bandow et al.[6] found as main products carbonyl compounds, dinitroxides, nitroxy-carbonyls, and nitroxy-alcohols. They made the first proposal of a reaction mechanism, which involves the formation of oxirane, although they had not detected it.

Wille et al.[7,8] identified the formation of oxirane at low pressures with a fast flow system and molecular beam sampling. They proposed a reaction mechanism where the oxirane is the main product, although the existence of other secondary pathways in which carbonyl compounds are formed as well is not ruled out.

Benter et al.[9] found a dependency of the oxirane concentration on the pressure and on the carrier gas. Using higher pressures and greater oxygen concentrations in the carrier gas increased the formation of peroxynitrates. However, at 1000 mbar, the oxirane yield was 75% in argon and 20% in air. A reaction mechanism in two steps was proposed. In the first one, the oxirane is formed, and in the second one, peroxynitrates are formed in the presence of oxygen.

Berndt et al.,[10,11] using a low flow system, studied the reaction of the NO_3 radical with several acyclic monoalk-

(1) Wayne, R. P.; Barnes, I.; Biggs, P.; Burrows, J. P.; Canosa-Mas, C. E.; Hjorth, J.; Bras, G. L.; Moortgat, G. K.; Perner, D.; Poulet, G.; Restelli, G.; Sidebottom, H. *Atmos. Environ.* **1991**, *25A*, 1.
(2) Atkinson, R. *J. Phys. Chem. Ref. Data* **1991**, *20*, 459.
(3) Atkinson, R.; Aschmann, S. M.; J. N. Pitts, J. *J. Phys. Chem.* **1988**, *92*, 3454.
(4) Morris, E. D. J.; Niki, H. *J. Phys. Chem.* **1974**, *78*, 1337.
(5) Japar, S. M.; Niki, H. *J. Phys. Chem.* **1975**, *79*, 1629.
(6) Bandow, H.; Okuda, M.;; Akimoto, H. *J. Phys. Chem.* **1980**, *84*, 3604.
(7) Wille, U.; Rahman, M. M.; Schindler, R. N. *Ber. Bunsen. Phys. Chem.* **1992**, *96*, 833.
(8) Wille, U.; Schindler, R. N. *Ber. Bunsen. Phys. Chem.* **1993**, *97*, 1447.
(9) Benter, T.; Liesner, M.; Schindler, R. N.; Skov, H.; Hjorth, J.; Restelli, G. *J. Phys. Chem.* **1994**, *98*, 10492.
(10) Berndt, T.; Bøge, O. *Ber. Bunsen. Phys. Chem.* **1994**, *98*, 869.
(11) Berndt, T.; Bøge, O. *J. Atmos. Chem.* **1995**, *21*, 275.

S0022-3263(98)00779-8 CCC: $15.00
Published on Web 09/17/1998

enes in synthetic air at the pressure of 1 bar. A reaction mechanism was suggested where there is a direct path from the adduct to the oxirane formation and another way in which the adduct is deactivated collisionally. Hence, this path is favored by increasing the pressure. Then, the final products would be oxirane, carbonyl compounds, or, through oxygen addition, peroxynitrates, ketones, and the radical HO_2.

Despite the obvious and general interest of these reactions, and the reliability of the quantum chemical methods to build proposals of reaction mechanisms, previous theoretical studies on this kind of reaction are scarce.[12]

In this work, we present a theoretical study of the mechanism of the reaction between the nitrate radical and the ethene molecule. The study has been carried out in several steps. First of all, a semiempirical study of the whole potential energy surface (PES) has been performed, and the stationary points have been classified according to their significance for this reaction. Then, these relevant stationary points, representing intermediate and transition state geometries, have been reoptimized, where possible, at ab initio ROHF[13] level, and then optimized again at CASSCF level of theory,[14] in order to have both geometries and energies calculated at a level as high as possible. In section 2 computational aspects are detailed. In section 3 a reaction mechanism is proposed and discussed. In section 3.1 the formation and characteristics of the initial adduct, common in the three found pathways, are presented. Section 3.2 describes the reaction pathway leading to epoxide formation, section 3.3 the pathway giving ethanal and ethenol, and section 3.4 the evolution of nitric acid. In section 3.5 the reaction energy profiles and the height of the energy barriers involved for all the reaction pathways studied are given. Finally, the main conclusions are enumerated in section 4.

2. Computational Details

Despite the small number of atoms involved, 10 atoms in total, the PES was very complex, involving many stationary points. Since we have kept the whole supermolecule as a doublet radical, the calculations involving geometry optimization, restricted when a transition state is studied, and vibrational analysis were too CPU time-consuming at ab initio level, and we have chosen to make a previous exploration of the PES at semiempirical level. AM1 method[15] was chosen, since it has been shown that it works well with radicals[16] and the agreement of AM1 geometries with experimental ones is generally satisfactory,[15] allowing to take them as starting point for further optimization at ab initio level.

We have then analyzed the stationary points obtained at AM1 level, and those points relevant for the studied reaction were chosen in order to build a draft of the reaction mechanism. Many other stationary points were dropped out, since they involved irrelevant movements, such as internal rotation of the CH_2 or NO_2 groups.

Taking the AM1 geometries as a starting point, we have reoptimized all the relevant stationary points at ROHF ab initio level,[13] unrestricted Hartree−Fock (UHF) giving SCF convergence problems. Only in one transition state have we not been able to completely optimize the geometry (see section 3.2). In this case, we optimized until a conformation as close to the true transition state as possible was obtained in the sense of maximizing the imaginary frequency associated to the reaction coordinate and minimizing the other imaginary frequencies.

The resulting ROHF geometries were further optimized at CASSCF[17−21] level. The active space was chosen as the minimum space which represents all the stationary points, resulting in a five electrons/six molecular orbitals active space. AM1 calculations were performed with the MOPAC 93 program[22] and ab initio ROHF and CASSCF calculations with the GAUSSIAN 94 series of programs.[23]

All the stationary points were fully optimized. In the three methods used in this theoretical study, AM1, ROHF, and CASSCF, the stationary points were characterized as minima or transition states by calculating the Hessian matrix and analyzing the vibrational normal modes. The eigenfollowing and transition state[24] methods have been used for the minima and transition states geometry optimizations, respectively.

At the ROHF level the Berny analytical gradient[25] was used for the minima and transition states geometry optimizations. Zero point correction has been calculated only with the CASSCF level. The basis set used was 6-31G*[26,27] which has polarization functions (d-type) on non-hydrogen atoms. Additional diffuse functions lead to convergence problems.

The active space was chosen in accord with a previous SDCI calculation choosing those orbitals with occupation numbers of 0.02 and 1.98.[28]

The calculations were performed on two IBM RS6000-590 computers, an IBM SP2, and a SGI Power Challenge L of the Theoretical Chemistry Group of the University of Valencia.

3. Results and Discussion

A reaction mechanism has been devised for the NO_3 + ethene reaction, starting from a critical revision of the

(12) Marston, G.; Monks, P.; Canosa-Mas, C.; R. P. Wayne. *J. Chem. Soc., Faraday Trans.* **1993**, *89*, 3899.
(13) Hurley, A. C. *Introduction to the Electron Theory of Small Molecules*; Academic Press: New York, 1976.
(14) Roos, B. In *Ab Initio Methods in Quantum Chemistry-II*; Lawley, K. P., Ed.; J. Wiley and Sons Ltd.: Chichester, 1987.
(15) Dewar, M. J. S.; Zoebisch, E. G.; Healy, F.; Stewart, J. J. P. *J. Am. Chem. Soc.* **1985**, *107*, 3902.
(16) Vinson, L.; J. J. Dannenberg. *J. Am. Chem. Soc.* **1989**, *11*, 2777.
(17) Hegarty, D.; Robb, M. A. *Mol. Phys.* **1979**, *38*, 1795.
(18) Eade, R. H. E.; Robb, M. A. *Chem. Phys. Lett.* **1981**, *83*, 362.
(19) Schlegel, H. B.; Robb, M. A. *Chem. Phys. Lett.* **1982**, *93*, 43.
(20) Bernardi, F.; Bottini, A.; McDougall, J. J. W.; Robb, M. A.; Schlegel, H. B. *Far. Symp. Chem. Soc.* **1984**, *19*, 137.
(21) Frisch, M. J.; Ragazos, I. N.; Robb, M. A.; Schlegel, H. B. *Chem. Phys. Lett.* **1992**, *189*, 524.
(22) J. J. P. Stewart. MOPAC 93. Technical report, Fujitsu Limited, Tokyo Japan 1993.
(23) Frisch, M. J.; Trucks, G. W.; Schlegel, H. B.; Gill, P. M. W.; Johnson, B. G.; Robb, M. A.; Cheeseman, J. R.; Keith, T.; Petersson, G. A.; Montgomery, J. A.; Raghavachari, K.; Al-Laham, M. A.; Zakrzewski, V. G.; Ortiz, J. V.; Foresman, J. B.; Cioslowski, J.; Stefanov, B. B.; Nanayakkara, A.; Challacombe, M.; Peng, C. Y.; Ayala, P. Y.; Chen, W.; Wong, M. W.; Andres, J. L.; Replogle, E. S.; Gomperts, R.; Martin, R. L.; Fox, D. J.; Binkley, J. S.; Defrees, D. J.; Baker, J.; Stewart, J. P.; Head-Gordon, M.; Gonzalez, C.; Pople, J. A. GAUSSIAN 94 revision d.3. Technical report, Gaussian Inc. Pittsburgh, PA, 1995.
(24) Baker, J. *J. Comput. Chem.* **1986**, *7*, 385.
(25) Schlegel, H. B. *J. Comput. Chem.* **1982**, *3*, 214.
(26) Hehre, W.; Radom, L.; Schleyer, P.; Pople, J. *Ab initio Molecular Orbital Theory*; Wiley-Interscience: New York, 1986.
(27) Hariharan, P.; Pople, J. *Chem. Phys. Lett.* **1972**, *16*, 217.
(28) Anglada, J.; Bofill, J. *Chem. Phys. Lett.* **1995**, *243*, 151.

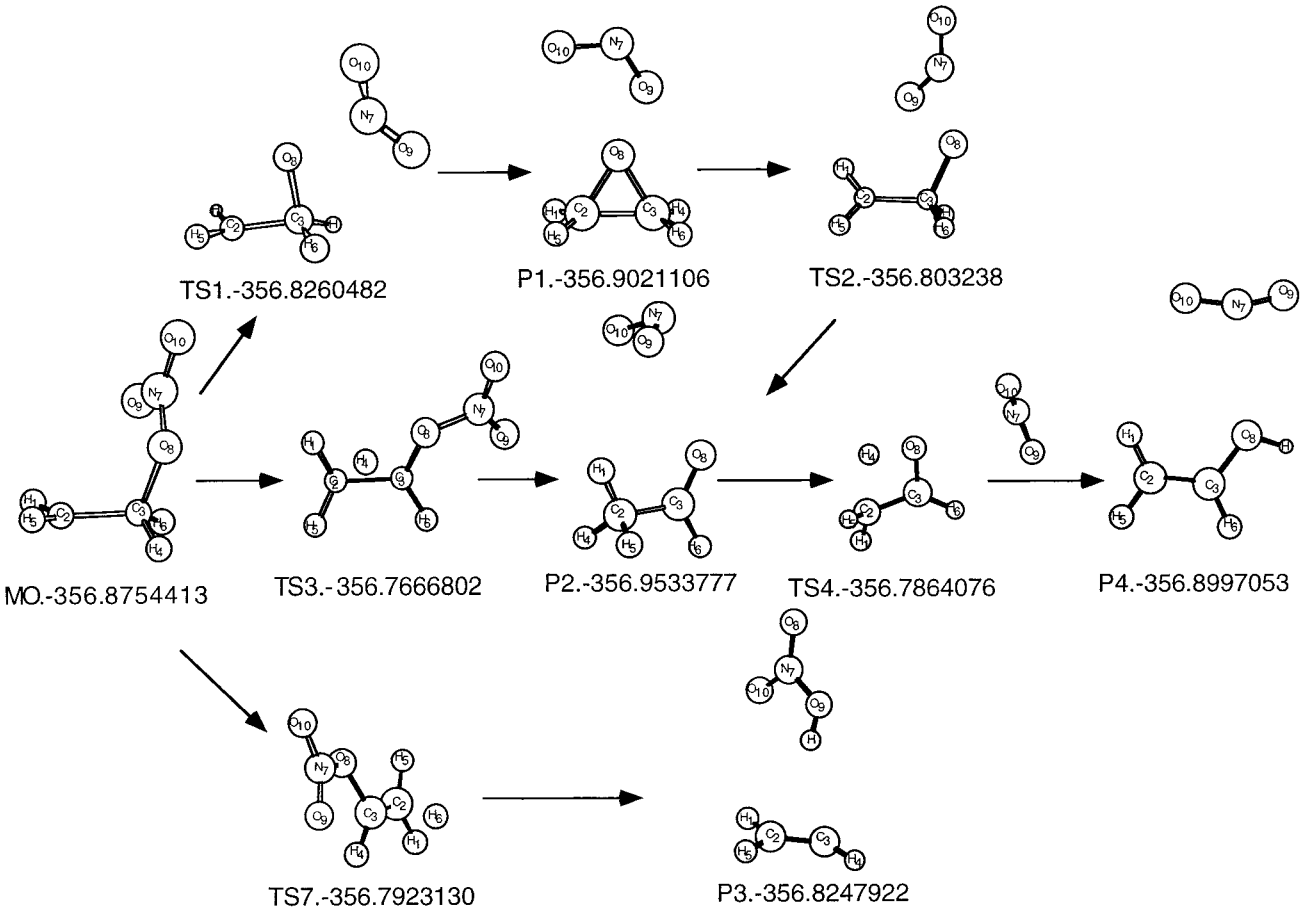

Figure 1. CASSCF(5,6)/6-31G* global reaction mechanism for the NO_3 + ethene addition reaction.

stationary points found at AM1 level. In the proposed reaction mechanism, only those stationary points related to a chemical reaction have been chosen. This means that only chemically different minima, and the saddle points connecting them, have been included in the reaction mechanism. Both geometries and energies of the selected stationary points have been eventually refined at ROHF and CASSCF levels of theory. In the reaction mechanism so obtained we have found three pathways leading to the following different main products: 1,2-epoxyethane, $CH_2(O)CH_2$, ethanal, CH_3CHO, and nitric acid, HNO_3. Other products found were the NO_2 radical and the vinyl, $CH_2CH^{\bullet}$, radical. The three pathways start from the same intermediate, a radical adduct which can be related to that mentioned in the experimental bibliography.[1] The global CASSCF reaction mechanism is depicted in Figure 1.

3.1. Initial Intermediate. The starting point in all three pathways, MO, has been characterized as a minimum in the PES with the three theoretical methods. No barrier has been found in the way leading from the reactant species at infinite distance until the MO adduct. In the resulting conformation for MO, the atom with the most negative charge is the C_2, so if an attack of an oxygen molecule takes place, it would oxidize the intermediate at the C_2 atom, producing peroxides, according to that reported experimentally.[29] The spin density is mainly localized in the C_2 atom. This fact confirms the experimental idea of an electrophilic addition to the double bond, and that when the double bond is more substituted, the reaction is favored due to the radical stabilization.

3.2. Epoxide Formation. In the three levels of theory, the first pathway of the reaction mechanism leads to the consecutive formation of oxirane, P1, and aldehyde, P2, as products, along with the NO_2 radical formation, through two saddle points, TS1 and TS2. Therefore, it involves five stationary points, whose optimized geometries are summarized in Table 1. The geometries for all the stationary points are very similar for CASSCF and ROHF methods, except for TS1. There are slight differences between AM1 and the two ab initio methods.

The transformation of the initial adduct, MO, in oxirane is carried out through a reaction coordinate involving the closure of the $C_2-C_3-O_8$ angle and the enlargement of the O_8-N_7 distance (see Figure 1). The transition state involved, TS1, has been characterized as a saddle point on the PES at both semiempirical and ab initio levels of theory. At AM1 and CASSCF levels, an imaginary frequencies of -963 cm^{-1} and -915 cm^{-1} were found, respectively. However, we have not been able to fully optimize it at ROHF level, due to an accidental degeneration of the HOMO, HOMO-1, and HOMO-2 orbitals. For this reason, multiconfigurational methods are needed to deal with this chemical situation. In all cases, the spin density spreads on the C_2 and N_7 atoms (see Figure 1). We have included the geometrical parameters in Table 1 corresponding to a conformation with three imaginary frequencies. The first one, at -1615 cm^{-1}, corresponds to the reaction coordinate, as described

(29) Barnes, I.; Bastian, V.; Becker, K. H.; Tong, Z. *J. Phys. Chem.* **1990**, *94*, 2413.

Table 1. Most Significant Geometrical Parameters in the Reaction Pathway Leading to Oxirane and Ethanal Formation at CASSCF, ROHF, and AM1 Levels[a]

parameter	method	MO	TS1	P1	TS2	P2
$r(C_2-C_3)$	CASSCF	1.488	1.481	1.453	1.490	1.504
	ROHF	1.488	1.433	1.452	1.459	1.503
	AM1	1.464	1.458	1.484	1.463	1.489
$r(O_8-C_3)$	CASSCF	1.449	1.392	1.403	1.430	1.190
	ROHF	1.450	1.390	1.405	1.306	1.190
	AM1	1.453	1.463	1.436	1.322	1.232
$r(O_8-C_2)$	CASSCF	2.449	2.048	1.403	2.425	2.390
	ROHF	2.449	1.770	1.405	2.252	2.387
	AM1	2.418	1.688	1.438	2.236	2.400
$r(N_7-O_8)$	CASSCF	1.333	1.985	3.049	3.275	3.172
	ROHF	1.329	1.697	2.832	2.555	2.889
	AM1	1.343	1.449	2.967	2.862	2.944
$r(H_4-C_2)$	CASSCF	2.222	2.164	2.198	2.148	1.086
	ROHF	2.137	2.194	2.194	2.100	1.087
	AM1	2.148	2.230	2.258	2.123	1.118
$\angle(O_8-C_3-C_2)$	CASSCF	112.9	90.9	58.8	112.4	124.7
	ROHF	112.9	77.7	58.9	109.0	124.5
	AM1	112.0	70.6	56.0	106.8	123.4

[a] Angles in degrees and distances in angstroms.

Table 2. Most Significant Geometrical Parameters in the Reaction Pathway Leading to Ethanal and Enol Formation at CASSCF, ROHF, and AM1 Levels[a]

parameter	method	MO	TS3	P2	TS4	P4
$r(C_2-C_3)$	CASSCF	1.488	1.472	1.504	1.421	1.333
	ROHF	1.488	1.462	1.503	1.416	1.314
	AM1	1.464	1.435	1.489	1.384	1.337
$r(O_8-C_3)$	CASSCF	1.449	1.400	1.190	1.254	1.363
	ROHF	1.450	1.397	1.190	1.256	1.357
	AM1	1.453	1.423	1.232	1.346	1.380
$r(H_4-C_2)$	CASSCF	2.222	1.343	1.086	1.539	3.130
	ROHF	2.137	1.300	1.087	1.514	3.116
	AM1	2.148	1.388	1.118	2.039	3.124
$r(H_4-C_3)$	CASSCF	1.079	1.330	2.135	1.611	1.915
	ROHF	1.079	1.280	2.131	1.596	1.912
	AM1	1.127	1.356	2.142	1.287	1.909
$r(O_8-H_4)$	CASSCF	1.965	3.368	3.093	1.255	0.945
	ROHF	1.965	2.309	3.089	1.239	0.945
	AM1	1.994	2.405	3.152	1.610	0.967
$\angle(H_4-C_3-C_2)$	CASSCF	111.7	57.1	28.6	60.6	148.5
	ROHF	111.7	55.9	28.7	60.0	149.4
	AM1	111.4	59.6	29.4	99.4	147.9

[a] Angles in degrees and distances in angstroms.

above. The other two imaginary frequencies, at −306 and −70 cm^{-1}, correspond to bending movements of the hydrogens.

The next point in the reaction mechanism, P1, has been characterized as a minimum on the PES. It represents the product experimentally found[7,8] in the global reaction, 1,2-epoxyethane along with the NO_2 radical. The path from TS1 to this product involves mainly the enlargement of the N_7-O_8 distance, and the O_8-C_3 and O_8-C_2 distances become nearly equal. The spin density due to the unpaired electron is located on the NO_2 radical fragment, mainly on the N_7 atom, according to that previously suggested.[30]

From oxirane a path exists leading to the formation of ethanal. The reaction coordinate involves the opening of the oxirane three-membered ring, a 1,2-hydrogen shift from C_3 to C_2, and the shortening of the C_3-O_8 bond, as this group becomes a carbonyl group. The saddle point involved, TS2, shows only an imaginary frequency of −615 cm^{-1} in AM1, −1005 cm^{-1} in ROHF and in CASSCF, associated with the opening of the ring. The spin density remains located on the NO_2 radical.

The final stationary point in this pathway is ethanal, P2, characterized as a minimum in the PES, although at CASSCF level a small imaginary frequency of −27 cm^{-1} appears, related to internal coordinates which give the relative positions of the two fragments, and that we have ruled out.[31] The path from TS2 to the aldehyde involves a 1,2-hydrogen shift from one carbon to another and the formation of the carbonyl group, the O_8-C_3 distance corresponding to then to a double bond.

3.3. Ethanal Formation. In the three levels of theory there is a second pathway in the reaction mechanism which goes directly to the formation of aldehyde, P2, and then to its enol, P4, giving also the NO_2 radical. This second pathway converges with the first one in the aldehyde, P2. The optimized geometries are summarized in Table 2. They are similar in the three methods, AM1 differing slightly from the two others.

The reaction coordinate leading to the aldehyde from the initial adduct involves a 1,2-hydrogen shift from the C_3 carbon atom to the C_2 (see Figure 1) and the enlargement of the O_8-N_7 bond length. In this reaction coordinate, the stationary point TS3 connecting the initial adduct, MO, to the aldehyde, P2, has been characterized as a transition state with a imaginary frequency of −2582 cm^{-1} in AM1, −3225 cm^{-1} in ROHF, and −2457 cm^{-1} in CASSCF, associated with the 1,2-hydrogen shift. Thus, the H_4-C_3 and H_4-C_2 distances are nearly equal. The spin density reflects this fact, since each carbon atom has nearly one-half of the total.

The formation of aldehyde, P2, is produced then by enlarging the O_8-N_7 distance and shortening the O_8-C_3 distance, to form the double bond in the carbonyl group. Along with P2, the NO_2 radical is formed.

Starting from the aldehyde, a path has been found that leads to the enol formation, P4. The reaction coordinate involves a hydrogen shift from the CH_2 group to the oxygen atom in the carbonyl group. The saddle point, TS4, connecting aldehyde and enol has been characterized as a transition state in the PES with an imaginary frequency of −1697 cm^{-1} in AM1, −2600 cm^{-1} in ROHF, and −2899 cm^{-1} in CASSCF, associated with the 1,2-H_4 shift.

The final stationary point on this pathway is the enol, P4, characterized as a minimum on the PES. To arrive at it from the previous transition state, the principal change is the shortening of the O_8-H_4 distance, to form the alcohol group, and of the C_3-C_2 distance to form the C═C double bond.

3.4. HNO_3 Formation. A third pathway has been found with the three methods leading to the formation of nitric acid and the vinyl radical. This pathway could have an important atmospheric implication, as it represents a contribution to the formation of acid rain. In the reaction coordinate three stationary points have been found. The optimized geometries are summarized in Table 3. The calculated values for the geometrical parameters are similar in the three methods.

The reaction coordinate involves a hydrogen transfer from the carbon atom toward a NO_3 terminal oxygen atom. The stationary point involved, TS7, connects MO with the nitric acid and the $CH_2CH\cdot$ radical. It has been characterized as a transition state in the PES with an imaginary frequency of −1684 cm^{-1} in AM1, −3035 cm^{-1}

(30) Dlugokencky, E. J.; J.Howard, C. *J. Phys. Chem.* **1989**, *93*, 1091.
(31) Hehre, W. J. *Practical Strategies for Electronic Structure Calculations*; Wavefunction, Inc: Irvine, CA, 1995.

Table 3. Most Significant Geometrical Parameters in the Reaction Pathway Leading to Nitric Acid Formation at CASSCF, ROHF, and AM1 Levels[a]

parameter	method	MO	TS7	P3
$r(C_2-C_3)$	CASSCF	1.488	1.358	1.330
	ROHF	1.488	1.339	1.307
	AM1	1.464	1.337	1.288
$r(O_8-C_3)$	CASSCF	1.449	1.391	5.235
	ROHF	1.450	1.395	5.183
	AM1	1.453	1.415	5.045
$r(H_6-C_3)$	CASSCF	1.077	1.857	2.580
	ROHF	1.077	1.650	2.515
	AM1	1.122	1.774	2.474
$r(O_9-H_6)$	CASSCF	2.393	2.849	0.958
	ROHF	2.391	2.775	0.961
	AM1	2.446	2.855	0.989

[a] Angles in degrees and distances in angstroms.

Table 4. AM1 Total Energy of Formation (eV) and ROHF and CASSCF Total Energy in (au)[a]

stationary points	AM1	ROHF	CASSCF
ethene	−310.36241	−78.0461642582	−356.8296142[a]
NO_3	−1161.91577	−278.745366769	
MO	−1474.47683	−356.875673869	−356.8754413
TS1	−1472.88340	−356.788468965	−356.8260482
P1	−1475.54028	−356.895317757	−356.9021106
TS2	−1472.85728	−356.761101944	−356.8032380
TS3	−1472.66856	−356.773986228	−356.7666802
P2	−1476.96076	−356.943676556	−356.9533777
TS4	−1472.59693	−356.798250633	−356.7864076
P4	−1476.50569	−356.912897736	−356.8997053
TS7	−1472.07225	−356.781033556	−356.7923130
P3	−1473.35373	−356.832560534	−356.8247922

[a] The energy of the reactant has been calculated as a supermolecule. CASSCF energy includes the zero point energy correction.

in ROHF, and −1230 cm^{-1} in CASSCF. The spin density is located on the H_6 and the C_2 atoms, with a proportion of 70/30, respectively, which can be associated to the movement of the H_6 atom.

Nitric acid and the vinyl radical are the final points on this pathway, P3. This is a stationary point, characterized as a minimum in the PES. This final step is reached by means of an hydrogen abstraction by one of the NO_3 oxygen atoms, as it is shown by the value of the O_9-H_6 distance which corresponds to a single bond. The spin density is located on the C_2 atom in the CH_2CH radical.

3.4. Reaction Profiles and E_a. The values for the CASSCF energies for all the stationary points studied are shown in Table 4. From these values, the energies relative to the ethene + NO_3 energy can be calculated for each stationary point. The relative energies are shown in Table 5. The reaction profiles, shown in Figure 2, have been calculated from the values in Table 5.

From the values of the relative energies we can explain most of the experimental evidences. Ethanal is the product thermodynamically more stable, and it would be the main product if the reaction control was thermodynamic. However, the lowest barrier to be overcome is that corresponding to TS1, leading to oxirane formation, which is the product found experimentally.[7,8] So, it can be said that this reaction is under kinetic control. The theoretical values for this barrier (see Table 5) are in agreement with the experimental activation energy. It must be pointed out that this barrier represents the highest energy barrier between the initial molecules

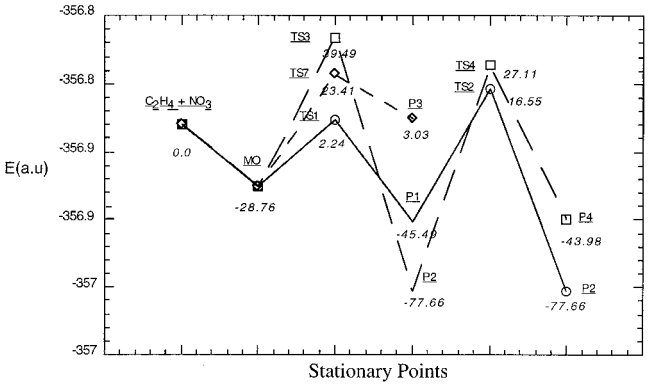

Figure 2. CASSCF(5,6)/6-31G* reaction profile of the addition reaction NO_3 + ethene.

Table 5. Energy Barriers in kcal mol^{-1} for the NO_3 + Ethene Reaction

	AM1	ROHF	CASSCF	experimental[1]
TS1 − (ethene + NO_3)	−13.96	1.92	2.24	6.17
TS3 − (ethene + NO_3)	−9.00	11.01	39.49	
TS7 − (ethene + NO_3)	4.75	6.59	23.41	
MO − (ethene + NO_3)	−50.70	−52.80	−28.76	
TS1−MO	36.74	54.72	30.99	
TS2−P1	61.87	84.22	62.04	
TS3−MO	41.69	63.81	68.25	
TS4−P2	100.30	91.25	104.78	
TS7−MO	55.30	59.39	52.16	
TS2−TS1	0.60	17.17	14.31	
TS4−TS3	1.65	−15.23	−12.38	
TS4−TS1	6.60	−6.15	24.87	
TS3−TS1	4.95	9.09	37.25	

(ethene and NO_3 radical) and the expected products of the whole reaction, oxirane and the NO_2 radical. It is thus the value to be compared with the experimental activation energy. The heights of the other barriers prevent the formation, either from MO or from oxirane, of ethanal, except for high temperatures. The formation of nitric acid can be discarded, since the barrier height involved is too high. The great stabilization energy of the initial adduct makes its formation very probable in the troposphere.

The reaction profile of the mechanism found at CASSCF is shown in the Figure 2 CASSCF. Stationary point individual energies and energy barriers between them at AM1, ROHF, and CASSCF are shown in Table 4. At AM1 level a negative E_a is obtained, contrary to prior experimental results, so the employment of ab initio methods was necessary. At ROHF and CASSCF the E_a is positive, and comparing with the experimental E_a, the CASSCF result is the best one of the three theory levels. This result is within the confidence margin of 0.5 eV. So, our mechanism has proved to be quantitatively correct. The energy barriers are quite different in the three methods, the CASSCF value being the smallest one.

4. Conclusions

A theoretical study of the addition reaction of the nitrate radical to ethene including geometry optimization and characterization of the stationary points at semiempirical, ROHF, and CASSCF correlated level, including five active electrons in six active orbitals, has been carried out. In the mechanism obtained, three different reaction pathways with different products have been localized, starting from the same intermediate, which can

be identified with the adduct suggested experimentally.[1] The products found are as follows: in the first pathway, oxirane and aldehyde; in the second reaction pathway, aldehyde and its enol; and in the third, nitric acid. This third reaction pathway can be discarded, on both a thermodynamical and kinetic basis.

Taking into account experimental data and the mechanism proposed in this work, we can conclude that, at low pressures 1,2-epoxyethane is the main product obtained, and the reaction is under kinetic control. However, at high pressures, the system could have enough energy to pass the barrier to form aldehyde. So, the main product would be oxirane, but a minor quantity of aldehyde could be formed, this pathway being of less importance. This mechanism would be in agreement with Wille et al.[7,8] and with the first part of the mechanism proposed by Berndt et al.[11]

Finally, the use of methods adequately able to take into account the nondynamic correlation is unavoidable when treating systems similar to those of this work, showing accidental degeneration between MO's, i.e., when bonds are breaking out and forming simultaneously. This fact is exemplified by the full optimization of the TS1 geometry at CASSCF correlated level, whereas it is impossible to do this at ROHF uncorrelated level of theory.

Acknowledgment. The authors thank Professor P. Viruela and M.Merchán for his kind and helpful suggestions and discussions. M.P.P thanks the Ministerio de Educación y Ciencia for a personal grant. This work was supported by Spanish DGICYT (project PB94-0993).

JO980779J